Synthesis of Wide-Band Planar Circulators Using Narrow Coupling Angles and Undersized Disk Resonators

Joseph Helszajn, *Senior Member, IEEE*, and Reinhard D. Baars, *Member, IEEE*

Abstract—**A drawback of the classic tracking solution exhibited by a junction circulator using a planar disk resonator is that it requires a wide coupling angle for its realization. This paper describes the theory of circulators using radial/lumped-element resonators with narrow coupling angles which display equally good, if not better, gyrator circuits that are outside of the classic result. The form of the lumped element variable is not unique and one way to realize it is to make use of the fringing capacitance at the interface between a dielectric resonator and a substrate with a higher relative dielectric constant than that of the resonator. The topology requires the adjustment of electromagnetic, electrostatic, and network conditions with common parameters so that a solution which relies on fringing effects only is not generally ensured. The paper includes the description of one such 1–2 GHz circulator.**

I. Introduction

The classic distributed circuit of a planar junction circulator is associated with certain interesting complex gyrator circuits which are suitable for the design of quarter-wave coupled circulators, but its implementation requires wide coupling angles (ψ) at the terminals of the resonator, a tensor permeability with an off-diagonal element (κ) bracketed between 0.50 and 1.0, and low values for the relative dielectric constant (ϵ_t) of the transformer region [1]–[8]. While many practical devices appear to respect this solution, many more apparently do not. One way to both overcome these shortcomings and to cater for this discrepancy is to replace the distributed resonator at the terminals of the junction by a mixed distributed-radial/lumped-element one. Such a hybrid resonator displays a $\psi, \kappa, kR, \omega, Q_L, B', G$ (coupling angle, off-diagonal element of the tensor permeability, radial wavenumber, frequency, loaded Q factor, susceptance slope parameter, gyrator conductance) space that contains circulation solutions that are outside of those of the conventional field, are exceptionally well behaved, have narrow coupling angles, and exhibit values of loaded Q factors that are compatible with the synthesis of quarter-wave coupled devices. However, some means of tuning the undersized resonator is necessary. This need may in some instances be met by making use of the fringing capacitance at the interface between the ferrite resonator and the substrate, a feature that is always, to some extent, present in the design of practical devices. The magnitude of this fringing capacitance is dependent upon both the thickness of the resonator and the relative dielectric constant of the substrate of the transformer region. Since both these quantities can in practice be varied by altering the topology of the matching network and the specification of the overall device, a range of practical solutions is in fact available. The saving grace in many experimental efforts is of course the fact that the network problem accommodates some uncertainty in the absolute level of the gyrator immittance provided the minimum ripple level of the specification is not tied down [9]. The theory of lumped element circulators is described in [10], and [11] and in certain papers on weakly magnetized devices [12]–[15].

The paper includes the synthesis of octave-band circulators using two quarter-wave-long impedance transformers. However, no attempt has been made to determine the optimum geometry. It also includes the experimental description of an octave-band device with a return loss of 20 dB which was partly experimentally adjusted prior to the development described here. The details of this device quantitively satisfy both the network and distributed variables of the junction and at first sight also meet the required lumped element part of the circuit. The use of effective magnetic walls to represent fringing effects in microstrip circuits is of course well understood [16]–[19] but its use is inappropriate in interpreting the complex gyrator circuit of many practical devices. The mixed form of the circuit employed here is necessary.

II. Complex Gyrator Circuits of Planar Circulators

The space described by the classic solution of a junction circulator using the simple planar disk resonator illustrated in Fig. 1 is usually fixed by two independent and one dependent variables. The two independent ones are the coupling angle (ψ) and the value of the off-diagonal element (κ) of the permeability tensor; the dependent variable is normally the radial wavenumber (kR). The region described by these three quantities contains a

Manuscript received December 12, 1989; revised April 24, 1991.
J. Helszajn is with the Department of Electrical and Electronic Engineering, Heriot-Watt University, Edinburgh, Scotland, U.K.
R. Baars is with UTE Microwave Inc., Asbury Park, NJ 07712.
IEEE Log Number 9102339.

0018-9480/91/1000-1681$01.00 ©1991 IEEE

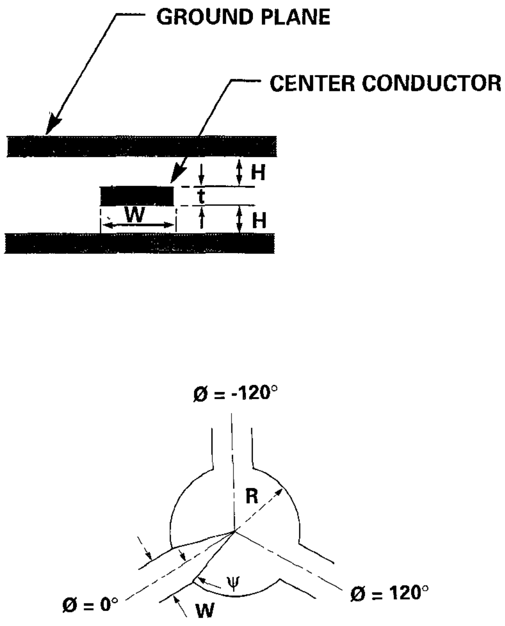

Fig. 1. Schematic diagram of stripline circulator.

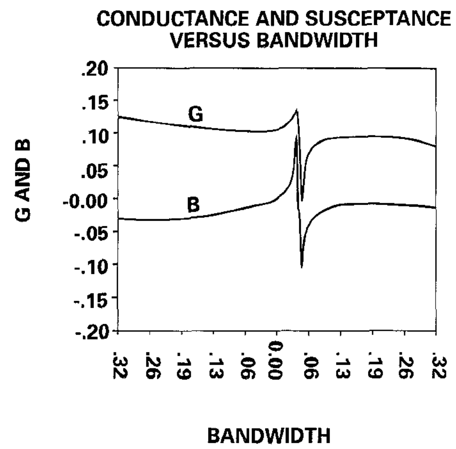

Fig. 2. Frequency response of complex gyrator circuit for $\psi = 0.25$, $\kappa = 0.67$, $kR = 1.99$, $Z_r = 50\ \Omega$, $\epsilon_f = 15$, and $\omega_0 C = 0$.

multiplicity of solutions, only some of which are well behaved over a particular frequency interval. One solution that is rather ill behaved is determined by ψ equal to, say, 0.25 rad and κ equal to, say, 0.67, for which the dependent variable, kR, is equal to 1.99. The frequency response of the complex gyrator circuit obtained with this boundary condition is illustrated in Fig. 2. The first six poles of the circuit have been retained in obtaining the data [3], [4].

The coupling angle entering into the description of this type of circuit is defined by

$$\psi = \sin^{-1}\left(\frac{W}{2R}\right) \tag{1}$$

and the impedance (Z_r) at the terminals of the resonator by

$$Z_r = 30\pi \ln\left[\frac{W + 2H + t}{W + t}\right]. \tag{2}$$

The radial wavenumber is defined by

$$kR = k_0\sqrt{(\epsilon_f \mu_{\text{eff}})}\, R \tag{3}$$

where

$$\mu_{\text{eff}} = \frac{\mu^2 - \kappa^2}{\mu}. \tag{4}$$

The normalized frequency variable δ is given by

$$\delta = \frac{\omega - \omega_0}{\omega_0}. \tag{5}$$

Here ω is the usual frequency variable (rad/s), ω_0 is the center frequency (rad/s), H is the thickness of each resonator (m), W is the width of the center conductor (m), R is the radius of the resonator (m), t is the thickness of the center conductor (m), k_0 is the free-space wavenumber (rad/m), ϵ_f is the relative dielectric constant of the garnet material, and μ_{eff} is its effective permeability. The parameters μ and κ are the diagonal and off-diagonal elements of the tensor permeability.

The frequency response in Fig. 2 has a characteristic resonance within its passband and is therefore, at first sight, of little value in the design of commercial devices. Although its character may be altered by varying either the coupling angle or the magnetic variables, the ensuing response will still, more often than not, be inadequate. Scrutiny of this problem indicates that, for $\psi < 0.26$ rad, kR exists only for $\kappa \leqslant 0.40$. For $\psi > 0.26$ rad, it exists for κ between 0 and 1. The classic wide-band solution is obtained with a unique coupling angle equal to $\psi = 0.53$ and a unique value for κ equal to 0.67 [3], [4]. Many practical devices, however, have equally suitable complex gyrator circuits that are outwith this condition. This common discrepancy between theory and practice may be understood by recognizing that practical devices seldom satisfy the ideal boundary conditions of the classic theory, which assumes an ideal magnetic wall everywhere on the periphery of the resonator except over the ports. In order to satisfy the open-wall condition it is necessary for the aspect ratio, R/H, of each resonator to be of the order of 5 or more and for the ratio of the relative dielectric constants of the garnet and the material in which it is embedded to be typically of the order of 10 or more.

III. Complex Gyrator Circuits of Planar Circulators Using Distributed-Radial/Lumped-Element Resonators

One way to cater for open walls in the description of a planar resonator is to replace it by an equivalent circuit with ideal walls but with effective parameters. Another is to retain the notion of a fringing capacitance in its description. The effect of such a composite resonator on the nature of the complex gyrator circuit of a junction circulator is the topic of this section. While both models can be equally well adjusted to describe the radial wavenumber of the resonator, the two need not exhibit similar reactance or susceptance slope parameters. The boundary

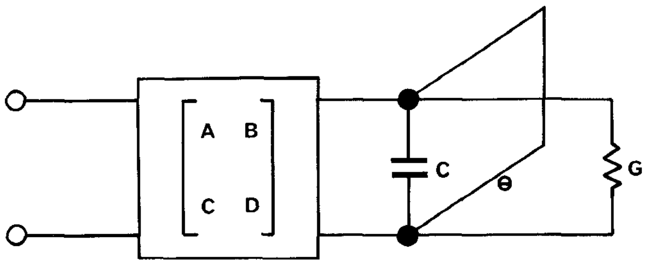

Fig. 3. Schematic diagram complex gyrator circuit using distributed–radial/lumped-element resonator.

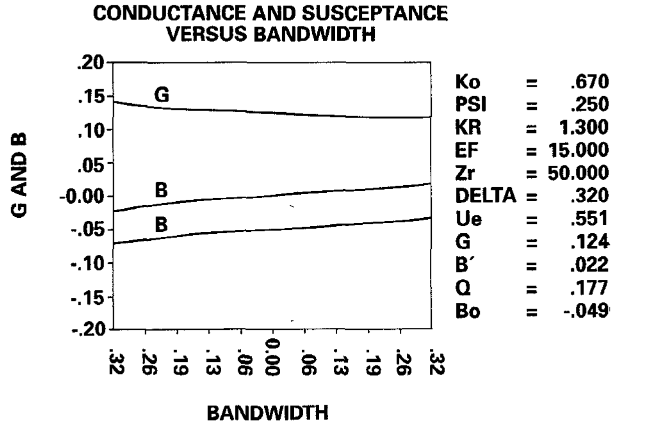

Fig. 4. Frequency responses of complex gyrator circuit for $\psi = 0.25$, $\kappa = 0.67$, $kR = 1.30$, $Z_r = 50\ \Omega$, $\epsilon_f = 15$ ($\omega_0 C = 0$ and 0.049(s)).

condition adopted here produces useful, new solutions and permits the radial wavenumber (kR) to be employed as an independent instead of a dependent variable. It is satisfied by replacing the conventional first circulation condition obtained by setting the imaginary part of the complex gyrator admittance to zero,

$$B_{\text{in}} = 0 \tag{6}$$

by

$$B_{\text{in}} + j\omega_0 C = 0. \tag{7}$$

B_{in} is the susceptance of the distributed disk circuit, $j\omega_0 C$ is that of a lumped capacitance at each port. C is separately written as

$$C(1+\delta). \tag{8}$$

The topology of the gyrator circuit in this instance is indicated in Fig. 3.

Fig. 4 indicates the real and imaginary parts of the distributed complex gyrator admittance for the parameters employed in obtaining the frequency response in Fig. 2 but with kR equal to 1.30. This equivalent circuit is well behaved over a considerable frequency interval but its resonant frequency is outside the range under consideration. It may, however, now be readily centered by adding a shunt lumped element susceptance at each port of the device in keeping with the condition in (7). Fig. 4 also displays the frequency response of such a hybrid junction. The response of this circuit is symmetrical about its center frequency and both its gyrator conductance and susceptance slope parameter are exceptionally well behaved over the frequency response of the device. It should therefore be of value in the synthesis of quarter-wave coupled devices.

TABLE I

κ_0	ψ	kR	B_0	G	B'	Q_L
0.500	0.200	1.3	0.086	0.123	0.089	0.724
0.500	0.250	1.3	0.067	0.100	0.074	0.733
0.500	0.300	1.3	0.055	0.089	0.058	0.752
0.525	0.200	1.3	0.082	0.128	0.080	0.628
0.525	0.250	1.3	0.064	0.105	0.067	0.638
0.525	0.300	1.3	0.052	0.090	0.058	0.652
0.550	0.200	1.3	0.079	0.133	0.071	0.536
0.550	0.250	1.3	0.061	0.109	0.060	0.547
0.550	0.300	1.3	0.049	0.093	0.052	0.562
0.575	0.200	1.3	0.076	0.138	0.062	0.449
0.575	0.250	1.3	0.058	0.113	0.052	0.460
0.575	0.300	1.3	0.046	0.097	0.046	0.476

Table I gives some (but not necessarily the best) circulation solutions for one choice of radial wavenumber. The first four entries in the table determine the boundary conditions of the junction and fix the first circulation condition of the circuit; the next three entries define the complex gyrator circuit of the device for the situation where $Z_r = 50\ \Omega$. The absolute value of the lumped element susceptance required to meet the first circulation condition is primarily dependent upon the choice of the radial wavenumber. The most significant parameter in the description of this kind of circuit is of course the value of the loaded Q factor displayed by the solution. This quantity fixes the gain–bandwidth of the device. The values displayed by the solutions tabulated here are in fact all suitable for the synthesis of devices with degree-3 equal ripple frequency responses over an octave band or more. Of some interest is the fact that the quality factor of the circuit increases as kR decreases. This would suggest that only a modest decrease in the radial wavenumber is sufficient to significantly alter the character of the complex gyrator circuit of the circulator. Such solutions are also associated with small values for the lumped element circuits. It is of separate note that the gyrator conductances displayed in these tables are essentially independent of the radial wavenumber. Another feature of the entries in the table is that both the susceptance slope parameter and the gyrator conductance decrease as the coupling angle increases. The ratio of these two quantities is the quality factor in the usual way.

IV. Complex Gyrator Admittance of Undersized Resonators

The complex gyrator admittance of one experimental junction using an undersized disk resonator at the junction of three 50 Ω air lines over the frequency interval 1.0 to 2.0 GHz and parametric values of the direct magnetic field is indicated in Fig. 5. The topology of this junction is described by a coupling angle (ψ) of 0.30 rad, an off-diagonal element (κ) with a nominal value of 0.70, a radial

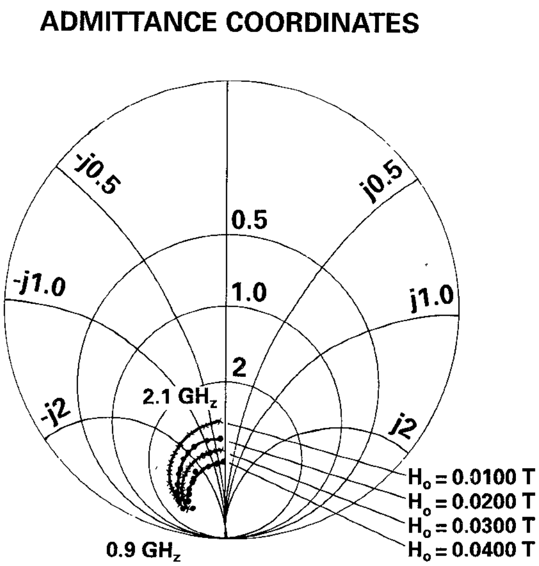

Fig. 5. Experimental Smith chart of undersized resonator ($kR = 1.2$, $\psi = 0.30$, $\kappa = 0.67$, $Z_r = 50\ \Omega$).

wavenumber (kR) of 1.21, and an aspect ratio of 2.77. The theoretical value of κ applies to a saturated material, a condition seldom established in practice. This result was obtained by decoupling port 3 from port 1 by placing a variable mismatch at port 2 [2]. It is observed from these data that the gyrator conductance and the susceptance slope parameter of the junction are nearly constant over the full experimental frequency interval. It also indicates that the magnitude of the real part intersects the theoretical value at approximately the direct field required to saturate the garnet material. The agreement between the theoretical and experimental values of the susceptance slope parameters (and therefore the loaded Q factors), while less good, is still gratifying. The value of the lumped element susceptance required to center the experimental data in Fig. 5 is likewise in keeping with that calculated in Table I. The slight deterioration in the complex gyrator circuit at the low-frequency extremity of the band is in part due to the onset of low-field loss and/or resonance loss.

V. Synthesis of Quarter-Wave Coupled Junction Circulators Using Distributed/Lumped Element Resonators

The physical design of quarter-wave coupled junction circulators with equal ripple frequency responses is not complete until both the network specification and the topology of the junction are stipulated. The network problem fixes the characteristic impedance (Z_r) at the terminals of the resonator and the relative dielectric constant (ϵ_t) of the transformer region in the normal way from a knowledge of the loaded Q factor and the relationship between the ripple specification and the bandwidth. The aspect ratio of the resonator (R/H) is also fixed once the coupling angle (ψ) and the impedance (Z_r) at the resonator terminals are stipulated. If the thickness of the center conductor is neglected, then the required relationship is

$$\frac{R}{H} = \frac{1}{\sin\psi\left[\operatorname{antiln}\left(\frac{Z_r}{30\pi}\right) - 1\right]}. \tag{9}$$

TABLE II

κ_0	ψ	kR	B_0	ϵ_t	R/H	W
0.500	0.200	1.3	0.086	15.9	4.85	0.760
0.500	0.250	1.3	0.067	10.4	5.35	0.755
0.500	0.300	1.3	0.055	7.5	5.72	0.748
0.525	0.200	1.3	0.082	20.0	3.58	0.819
0.525	0.250	1.3	0.064	13.1	3.99	0.812
0.525	0.300	1.3	0.052	9.4	4.32	0.804
0.550	0.200	1.3	0.079	24.9	2.20	0.884
0.550	0.250	1.3	0.061	16.4	2.57	0.875
0.550	0.300	1.3	0.049	11.7	2.88	0.864
0.575	0.200	1.3	0.076	30.5	1.43	0.954
0.575	0.250	1.3	0.058	20.1	1.74	0.945
0.575	0.300	1.3	0.046	14.4	2.02	0.931

Table II summarizes some network solutions corresponding to the entries in Table I for the case of a topology employing two quarter-wave-long impedance transformers. The first three entries are therefore common in the two tables; the next two entries specify the relative dielectric constant of the transformer region and the aspect ratio of the resonator. These quantities are not unique but are dependent upon the network specification. The entries in this table satisfy the network problem with $S(\min) = 1.05$ and $S(\max) = 1.15$ over one octave band or more. Fairly large values for the relative dielectric constant of the transformer region, narrow coupling angles (in contrast to the conventional solution), and practical ground plane spacings are features of these solutions. Scrutiny of the network problem indicates that quite small changes in the ripple specification can produce fairly large variations in both these quantities. The last entry in Table II is the bandwidth for the ripple level adopted. The only entries that need to be considered in these tables are those for which R/H leads to practical ground plane spacings (say, $1.5 \leqslant R/H \leqslant 4$).

Fig. 6 depicts the frequency responses of the gyrator circuit over an 80% band for one situation without and with lumped element susceptances at each port. Fig. 7 indicates the frequency response of a degree-3 quarter-wave coupled device using this solution. The aspect ratio of this resonator is 2.75, the radial wavenumber is 1.40, and the value of the lumped susceptance is 0.0557 S. The relative dielectric constant of the transformer region is 16.7. The classic solution is described by $\kappa = 0.67$, $\psi = 0.53$, and $kR = 1.57$ [3].

The required form of the lumped element discontinuity at the resonator terminals is not unique and may be obtained in a number of different ways. One way it may be fully or partially realized is by absorbing the fringing capacitance at the open wall of the resonator into the

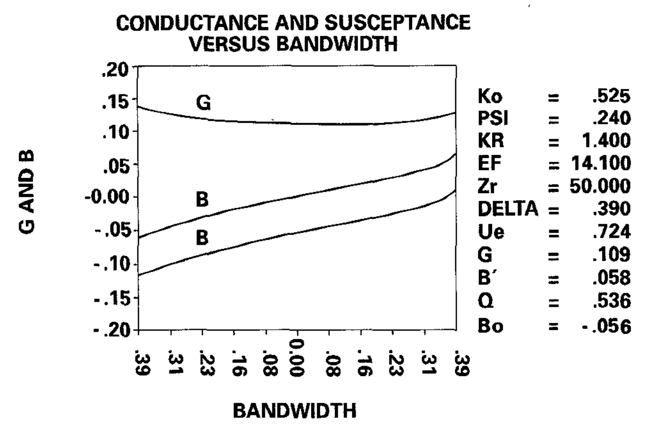

Fig. 6. Frequency responses of complex gyrator circuit for $\psi = 0.24$, $\kappa = 0.525$, $kR = 1.40$, $\omega_0 C = 0$, $Z_r = 50\ \Omega$ ($\omega_0 C = 0$ and 0.056).

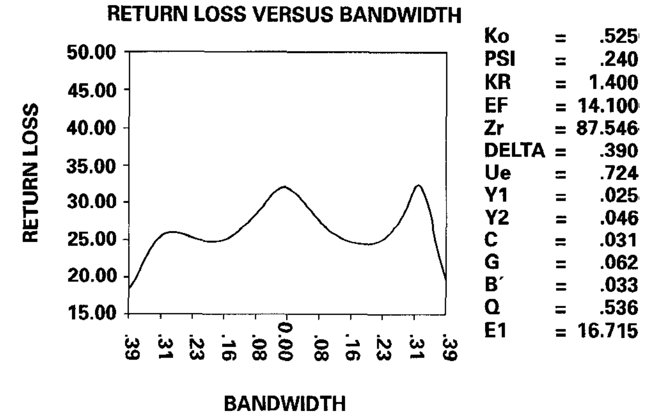

Fig. 7. Frequency response of two quarter-wave coupled junction for $\psi = 0.24$, $\kappa = 0.525$, $kR = 1.4$, and $\omega_0 C = 0.056$.

design. This sort of capacitance arises naturally in the design of quarter-wave coupled devices, since the impedance level of the transformer section adjacent to the junction is usually realized by loading the free-space impedance defined by the resonator terminals with a material with an appropriate dielectric constant. Its value is, however, a function of both the aspect ratio (R/H) of the resonator and the relative dielectric constant of the substrate at the boundary of the open resonator. Since these quantities are not fixed until the specification is spelled out (see Table I), a solution to the characteristic equation which is compatible with the network problem is therefore not at first sight ensured. Preliminary scrutiny of this problem and the practical device described in the next section suggests that it can by itself essentially provide a means of realizing mixed distributed–radial lumped-element resonators that are compatible with the construction of at least one class of octave-band circulator.

VI. Mixed Radial–Distributed/ Lumped-Element Resonator

In order to quantify the practical loading of the open wall of a ferrite or garnet resonator embedded in a dielectric substrate, some dedicated measurements have

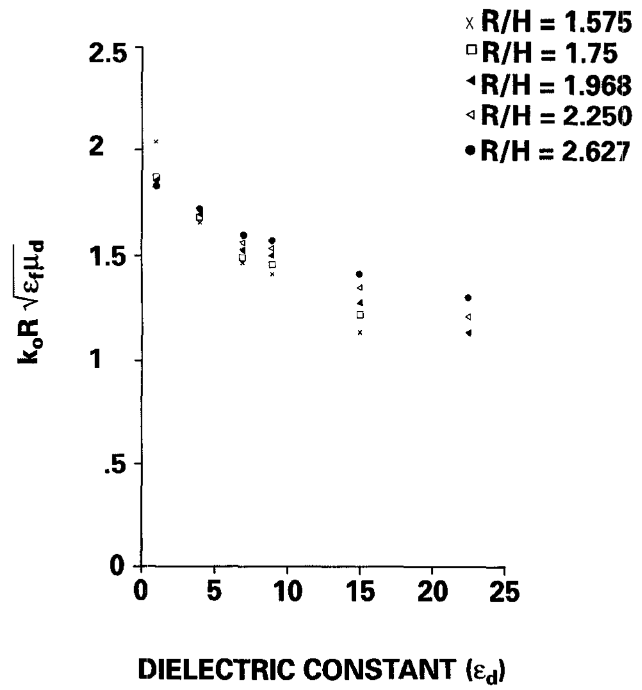

Fig. 8. Resonant frequency of loosely coupled stripline resonator embedded in dielectric substrate.

been undertaken. Fig. 8 depicts the radial wavenumber ($k_0 R \sqrt{\epsilon_f \mu_d}$) of the dominant mode of a loosely coupled garnet resonator embedded in a medium with a relative dielectric constant ϵ_d for parametric values of R/H. This result indicates a pronounced dependence of the radial wavenumber upon both the aspect ratio of the resonator and the relative dielectric constant of the substrate. The perturbation of the wavenumber is especially significant if the relative dielectric constant of the substrate material is comparable to or larger than that of the garnet resonator and if the aspect ratio of the resonator is bracketed by $1.5 \leqslant R/H \leqslant 4.0$.

The influence of the demagnetized permeability of the gyromagnetic resonator has not been embodied in these data. It is defined by

$$\mu_d = \frac{1}{3} + \frac{2}{3}\left[1 - \left(\frac{\gamma M_0}{\mu_0 \omega}\right)^2\right]^{1/2} \tag{10}$$

where γ is the gyromagnetic constant (2.21×10^5 (rad/s)/(A/m)), μ_0 is the free-space permeability ($4\pi \times^{-7}$ H/m), and ω is the usual radian frequency (rad/s). The magnetization (M_0) employed in this work is 0.0400 T.

VII. 1–2 GHz Device

Scrutiny of the experimental frequency response of the complex gyrator circuit in Fig. 5 indicates that in order to center it its radial wavenumber must be lowered by a factor of about 0.75. One way this may be achieved is by loading each of its terminals by a lumped susceptance equal to about 0.06 (S). Another possibility is to make use of the fringing capacitance at the boundary between a disk resonator and a suitable dielectric substrate. A solution to this problem is not ensured, but inspection of Fig. 8 indicates that constant R/H curves between 1.75 and 2.62 provide a number of such solutions for ϵ_d between 15 and 25. Some possible theoretical entries that are suitable for the design of a wide-band device which straddles these physical parameters except for the value of κ are given by the entries in row seven in Tables I and II. A perusal of Figs. 5 and 8 separately indicates that this solution approximately satisfies the first circulation solution of the circulator.

Any discrepancy between the required discontinuity and that displayed by the junction may in practice be accommodated by loading the junction with appropriate magnetic walls [20]. Scrutiny of Fig. 8 also suggests, once the radial wavenumber is adjusted for the omission of the effective permeability, that the required fringing susceptance is also nearly naturally met in (2) by the solution summarized by Figs. 6 and 7.

The ratio of the demagnetized and effective radial wavenumbers is

$$\frac{k_0 R\sqrt{\epsilon_f \mu_d}}{kR} = \sqrt{\frac{\mu_d}{\mu_{\text{eff}}}}. \tag{11}$$

A 1–2 GHz device based on the topology outlined here (using the junction described in connection with Fig. 5) has in fact been partly experimentally developed prior to the theory outlined here and optimized thereafter. It is described by

$$\psi \approx 0.27$$
$$\kappa \approx 0.70$$
$$kR \approx 1.21$$
$$R/H = 2.77$$
$$\epsilon_d = 25.$$

The discrepancy between the two values of the normalized magnetization (κ) of the garnet material may be understood by recognizing that its value at magnetic saturation (κ) represents in practice an upper bound on its actual value (κ'). The two values of the normalized magnetization are related by

$$\kappa' = \left(\frac{M}{M_s}\right)\kappa$$

where M is the actual magnetization of the material, and M_s is its value at magnetic saturation. If M is taken as the remanence value of the hysteresis of the material loop, then

$$\frac{M}{M_s} \approx 0.70$$

and the value of κ' in this example is consistent with those appearing in Table I.

Fig. 9 illustrates a typical response at one port of the device. Some fine trimming of the junction or the fringing capacitance with the aid of transverse magnetic walls [20] in the manner indicated in Fig. 10 was employed in obtaining this result; otherwise all the variables utilised in this work were within 15% of the theoretical values. The insertion loss between any two ports was less than 0.35 dB over the full frequency interval.

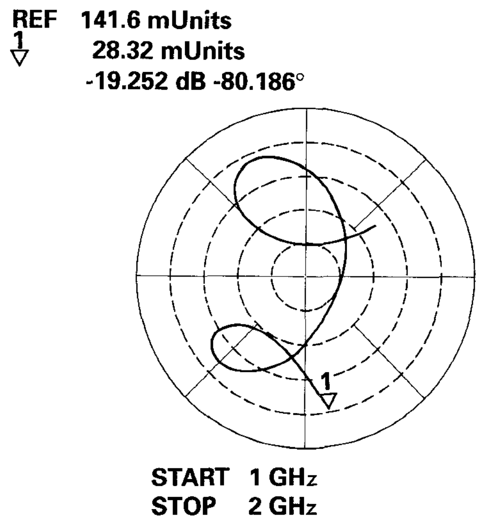

Fig. 9. Frequency response of two quarter-wave-long transformer coupled junction using mixed radial–distributed/lumped-element resonator.

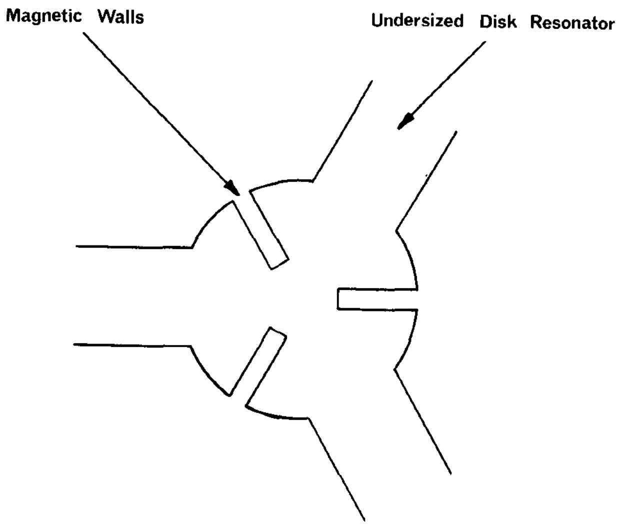

Fig. 10. Schematic diagram of disk resonator loaded with magnetic walls.

VIII. Conclusions

Mixed distributed–radial/lumped element resonators may be adjusted to exhibit exceptionally well behaved equivalent circuits that are suitable for the synthesis of practical wide-band circulators. One way to realize the lumped element term is to embody the fringing capacitance at the terminals of a resonator embedded in a substrate with a higher relative dielectric constant than that of the resonator in the design. The paper describes a 1–2 GHz device based on one such a solution with an insertion loss of no more than 0.35 dB between any two ports and a typical return loss of 20 dB.

Acknowledgment

The authors would like to thank D. Galloway at UTE Microwave, NJ, for some of the experimental work.

References

[1] J. B. Davies and P. Cohen, "Theoretical design of symmetrical junction stripline circulators," *IEEE Trans. Microwave Theory Tech.*, vol. MTT-11, pp. 506–512, Nov. 1963.
[2] J. W. Simon, "Broadband strip-transmission line Y-junction circulators," *IEEE Trans. Microwave Theory Tech.*, vol. MTT-13, pp. 335–345, May 1965.
[3] Y. S. Wu and F. J. Rosenbaum, "Wideband operation of microstrip circulators," *IEEE Trans. Microwave Theory Tech.*, vol. MTT-22, pp. 849–856, Oct. 1974.
[4] J. Helszajn, "Operation of tracking circulators," *IEEE Trans. Microwave Theory Tech.*, vol. MTT-29, pp. 700–707, July 1981.
[5] R. W. Lyon and J. Helszajn, "A finite element analysis of planar circulators using arbitrarily shaped resonators," *IEEE Trans. Microwave Theory Tech.*, vol. MTT-30, pp. 1964–1974, Nov. 1982.
[6] T. Miyoshi and S. Miyaushi, "The design of planar circulators for wideband operation," *IEEE Trans. Microwave Theory Tech.*, vol. MTT-28, pp. 210–215, Mar. 1980.
[7] J. Helszajn, "Contour-integral formulation of complex gyrator admittance of junction circulators using triangular resonators," *Proc. Inst. Elec. Eng.*, vol. 132, pt. H, pp. 255–269, July 1985.
[8] Y. Ayashi, "Analysis of wideband stripline circulators for wideband operation," *IEEE Trans. Microwave Theory Tech.*, vol. MTT-28, pp. 210–214, 1980.
[9] R. Levy and J. Helszajn, "Specific equations for one and two section quarter-wave matching networks for stub-resistor loads," *IEEE Trans. Microwave Theory Tech.*, vol. MTT-30, pp. 55–62, Jan. 1982.
[10] V. E. Dunn and R. W. Roberts, "Miniature VHF and UHF circulators use lumped element design," *Microwaves*, pp. 46–47, Dec. 1963.
[11] Y. Konishi, "Lumped element Y circulator," *IEEE Trans. Microwave Theory Tech.*, vol. MTT-13, pp. 852–964, 1965.
[12] U. Milano, J. H. Saunders, and L. Davis, Jr., "A Y-junction stripline circulator," *IRE Trans. Microwave Theory Tech.*, vol. MTT-8, pp. 346–351, 1960.
[13] H. Bosma, "On stripline Y-circulation at UHF," *IEEE Trans. Microwave Theory Tech.*, vol. MTT-12, pp. 61–72, Jan. 1964.
[14] C. E. Fay and R. L. Comstock, "Operation of the ferrite junction circulator," *IEEE Trans. Microwave Theory Tech.*, vol. MTT-13, pp. 15–21, Jan. 1965.
[15] J. Helszajn, "Quarter-wave coupled junction circulators using weakly magnetized disk resonators," *IEEE Trans. Microwave Theory Tech.*, vol. MTT-30, pp. 800–806, May 1982.
[16] C. H. Oxley, T. J. Brazil, J. J. Purcell, and R. Genner, "Design and performance of J band ferrite microstrip circulators," *Proc. Inst. Elec. Eng.*, vol. 125, no. 8, Aug. 1978.
[17] T. Itoh and R. Mittra, "Analysis of a microstrip disk resonator," *Arch. Elektron Übertragungs.*, vol. 27, pp. 456–458, 1973.
[18] I. Wolff and N. Knoppik, "Rectangular and circular disk capacitors and resonators," *IEEE Trans. Microwave Theory Tech.*, vol. MTT-20, pp. 857–864, 1974.
[19] W. T. Nisbet and J. Helszajn, "Mode charts for microstrip resonators on dielectric and magnetic substrates using a transverse resonance method," *Proc. Inst. Elec. Eng.*, pt. H (*Microwaves, Opt. and Acoust.*), pp. 69–77, 1979.
[20] J. Helszajn, R. Baars, and W. T. Nisbet, "Characteristics of circulators using planar triangular and disk resonators symmetrically loaded with magnetic walls," *IEEE Trans. Microwave Theory Tech.*, vol. MTT-28, June 1980.

Joseph Helszajn (M'64–SM'87) was born in Brussels, Belgium, in 1934. He received the Full Technological Certificate of the City and Guilds of London Institute from Northern Polytechnic, London, England (1955), the M.S.E.E. degree from the University of Santa Clara, CA (1964), the Ph.D. degree from the University of Leeds, Leeds, England (1969), and the D.Sc. degree from Heriot-Watt University, Edinburgh, Scotland (1976).

He has held a number of positions in the microwave industry. From 1964 to 1966, he was Product Line Manager at Microwave Associates, Inc., Burlington, MA. He is now Professor of Microwave Engineering at Heriot-Watt University. He is the author of the books *Principles of Microwave Ferrite Engineering* (New York: Wiley, 1969), *Nonreciprocal Microwave Junctions and Circulators* (New York: Wiley, 1975), *Passive and Active Microwave Circuits* (New York: Wiley, 1978), *YIG Resonators and Filters* (New York: Wiley, 1985), *Ferrite Phase Shifters and Control Devices* (London, McGraw-Hill, 1989), *Synthesis of Lumped Element, Distributed and Planar Filters* (London, McGraw-Hill, 1990), and *Passive, Active and Nonreciprocal Microwave Circuits* (London, McGraw-Hill, 1991).

Dr. Helszajn is a Fellow of the Institute of Electrical Engineers. In 1968, he was awarded the Insignia Award of the City and Guilds of London Institute. He is an Honorary Editor of *Microwaves, Antennas and Propagation* (*IEE Proceedings*).

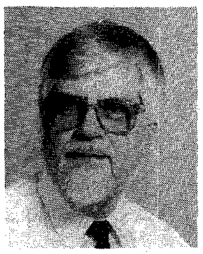

Reinhard D. Baars (S'58–M'59) was born in Marburg/Lahn, Germany, in 1934. He received the B.S.E.E. and M.S.E.E. degrees from the New Jersey Institute of Technology (Newark College of Engineering, Newark, NJ) in 1958 and 1965, respectively.

He has held a number of engineering and management positions with manufacturers of various microwave components. His field of specialization has been in the areas of ferrite devices and filters, both coaxial and waveguide. He has served as Vice President of Engineering and Manufacturing for UTE Microwave, Inc., Asbury Park, NJ, since that company's inception, in 1972.